Palaeogeography, Palaeoclimatology, Palaeoecology 512 (2018) 71–79

Contents lists available at ScienceDirect

Palaeogeography, Palaeoclimatology, Palaeoecology

journal homepage: www.elsevier.com/locate/palaeo

Linkage between Lake Xingkai sediment geochemistry and Asian summer monsoon since the last interglacial period

Weiwei Sun[a,*], Enlou Zhang[a], Enfeng Liu[b], Jie Chang[a], Ji Shen[a,c,**]

[a] State Key Laboratory of Lake Science and Environment, Nanjing Institute of Geography and Limnology, Chinese Academy of Sciences, Nanjing 210008, China
[b] College of Geography and Environment, Shandong Normal University, Jinan 250014, China
[c] College of Earth Sciences, University of Chinese Academy of Sciences, Beijing 100049, China

ARTICLE INFO

Keywords:
Chemical weathering
Sediment recycling
Sorting
Physical erosion
Lake Khanka
Northeast China

ABSTRACT

In this study, we present the element geochemical data of Core XK08-A2 drilled from Lake Xingkai (Khanka), northeast China. The study aims to examine the changes of sediment provenance and geochemical composition in response to Asian summer monsoon variability since the last interglacial period. Major elemental analyses on lacustrine samples and sand samples from Lake Xingkai and the surrounding sandy ridges in northeast China indicate that their abundance varied in relatively narrow ranges. The samples had only undergone the primary stage of chemical weathering. Similar Ti/Al and K/Al ratios between the lacustrine samples from Lake Xingkai and the loess-paleosol samples in north China were observed, which suggests that they come from broadly similar desert sources. Due to the significant dependence on grain-size and influence of sediments recycling, Chemical Index of Alteration of the lacustrine sediments could not be regarded as sensitive indicators of source regions' weathering on the glacial-interglacial timescale. Alternatively, the geochemical proxies of the lacustrine sediments could be linked to the Asian summer monsoon through the development of runoff and physical erosion in the catchment. Weakened Asian summer monsoon caused more fine particles transported to the lake basin by reduced runoff in the last glacial period. In contrast, coarser and less-weathered detritus are transported into the lake accompanying strengthened Asian summer monsoon during the warm periods.

1. Introduction

On geological timescales, chemical weathering of silicates on the continent plays a significant role in many surface processes, including the regulation of global carbon cycling and modification of ecosystem structure by controlling nutrients availability into oceans, lakes and soil surfaces (Nesbitt and Young, 1982; Rogers et al., 1998; Kump et al., 2000). Variations of chemical weathering intensity in the past are inferred from archives such as aeolian sediments (Chen et al., 1999; Yang et al., 2006; Li et al., 2008; Xiong et al., 2010), lacustrine sediments (Jin et al., 2001; Selvaraj et al., 2007; An et al., 2011; Liu et al., 2014; Jin et al., 2015), and marine sediments (Hu et al., 2012; Clift et al., 2014; Zhao et al., 2017). Geochemical and mineralogical proxies for chemical weathering intensity have been well-developed, for example, Rb/Sr ratio (Chen et al., 1999; An et al., 2011; Jin et al., 2015), strontium isotopes (Yang et al., 2000), Chemical Index of Alteration (CIA) (Xiong et al., 2010; An et al., 2011), and illite/chlorite ratio (Zhao et al., 2005). Multi-proxy records from the Chinese Loess Plateau generally suggest that chemical weathering is favored under warm-wet conditions in the interglacial periods, and the weak weathering intensity is found during glacial periods (Chen et al., 1999; Yang et al., 2000; Yang et al., 2006; Li et al., 2008). However, the results from lacustrine and marine sediments indicate that the weathering intensities respond to climate change differently in both temporal and spatial distribution. For example, An et al. (2011) suggested that higher CIA values of lacustrine sediments from Heqing basin in southwest China represent strong chemical weathering, reflecting strengthened Indian summer monsoon, while in Taiwan Island, low CIA values and strengthened physical weathering correspond to warm and humid climate (Selvaraj et al., 2007; Zhao et al., 2017). However, a few studies have addressed the problem of whether geochemistry of sediments is influenced by recycling and inheritance from previous sedimentary cycles (Yang et al., 2004; Yang et al., 2006; Garzanti et al., 2013).

Northern China lies in the mid-high latitudes of the Eurasia continent and is influenced by the interaction between Asian monsoon circulation system and polar climate systems. The region is particularly

* Corresponding author.
** Corresponding author at: State Key Laboratory of Lake Science and Environment, Nanjing Institute of Geography and Limnology, Chinese Academy of Science, Nanjing 210008, China.
E-mail addresses: wwsun@niglas.ac.cn (W. Sun), jishen@niglas.ac.cn (J. Shen).

https://doi.org/10.1016/j.palaeo.2018.06.026
Received 29 January 2018; Received in revised form 7 June 2018; Accepted 14 June 2018
Available online 20 June 2018
0031-0182/

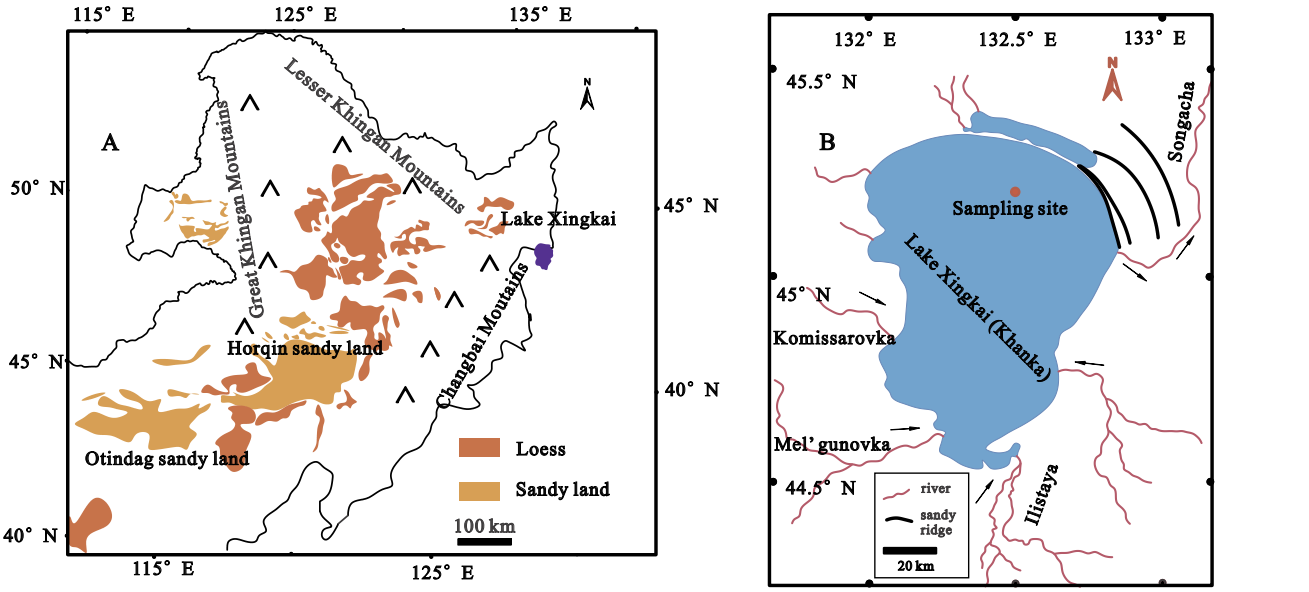

Fig. 1. Map of study region showing the distribution of loess and sandy lands in northeast China, and the locations of Lake Xingkai (A) and location of coring site (B).

sensitive to changes in the monsoonal intensity (Shen, 2013). Some authors suggest that the geochemical indices of lacustrine sediments could be used to reconstruct the silicate chemical weathering history (Jin et al., 2001; Ao et al., 2010; Cai et al., 2014; Jiang et al., 2016). However, important dust sources are distributed in the arid inland basins in the northwest China, and the dust emission to the atmosphere could be transported for thousand kilometers (Uno et al., 2009). Some part of dust particles also deposited into the lake bottom directly in middle latitudes of the Northern Hemisphere (Xiao et al., 1999; Liu et al., 2009; F. Chen et al., 2013; Jin et al., 2015; Sun et al., 2018). The possible influences of sediment sources and transporting dynamics change on the geochemical evolution of lacustrine sediments during the late Quaternary have rarely been investigated in this region.

In this study, we present a geochemical record since the last interglaciation from Lake Xingkai (Khanka) in the boundary of China and Russia (44°32′–45°21′N, 131°58′–132°51′E, Fig. 1A). The lake is the only site in this region that were chosen for global lake drilling points in the Past Global Changes Pole-Equator-Pole program due to its key position (Williams et al., 2001). The objectives are first to distinguish the provenance of the lacustrine sediment; then to evaluate the effects of recycling and sorting on sedimentary chemical weathering degree; and further to clarify the influence of sedimentary processes on silicate weathering reconstruction.

2. Regional setting

Northeast China is characterized by plains and sand fields separated by three major mountain systems: The Great Khingan Mountains, Lesser Khingan Mountains and Changbai Mountains. Loess deposits in Northeast China are also widely distributed in eastern Inner Mongolia, downwind of the Horqin and Otindag sandy deserts (Fig. 1A). Lake Xingkai is the largest freshwater lake in northeastern Asia, with a surface area of 4190 km^2 and a catchment of 16,890 km^2. The lake basin is situated in the Jiamusi-Khanka Massif, which is surrounded by Nadanhada Terrane and the Sikhote- Alin accretionary complex belt to the east, the Mongolia- Okhotsk suture zone and Songliao terrane to the west (Yang et al., 2015). The bedrock is dominated by Paleozoic granulite facies, amphibolite facies and granitoids. In addition, Mesozonic- Cenozoic volcanic sedimentary assemblages also occur in the region (Yang et al., 2015). The lake basin is filled by Quaternary sediments of 200 m thick (Wan and Zhong, 1997). The lake is mainly fed by the Komissarovka, Mel'gunovka, Ilistaya and Spasovka Rivers in Russia and the Baileng River in China. It has only one outflowing river (i.e., the Songacha River) in the northeast, which flows into the Ussuri River (Fig. 1B). On the north side of the lake, there are four sandy ridges located in parallel concentric arcs with the lake present shoreline (Fig. 1B, Zhu et al., 2011; Long and Shen, 2017). The sandy ridges were mainly composed of rounded sands with a dominated mode of 200–500 μm, which suggested that the particles are recycled from the nearshore region when the lake level was low (Zhu et al., 2011; Long and Shen, 2017).

The climate of the lake basin is controlled by cold, continental Serbian- Mongolian highs in winter, and by warmer and moisture air originated from the low latitudes in summer (Shen, 2013; Long et al., 2015). The maximum monthly mean temperature is about 21 °C in July and the minimum monthly mean temperature is about −18 °C in January inferred from the instrumental data available from the adjacent meteorological station. Rainfall was brought by the Asian summer monsoon from June to September which accounts for about 70% of the mean annual precipitation (~540 mm). The lake is covered by ice from the late October to the April.

3. Materials and methods

3.1. Field work and sample dating

In the summer of 2008, two parallel sediment cores (308-cm-long XK08-A1 and 336-cm-long XK08-A2) were retrieved using a UWITEC piston corer near the China-Russia boundary (Fig. 1b, 45°12′21″N, 132°30′33″ E). The water depth was about 7.0 m. Sands from the sandy ridges were also sampled during the field work to represent the bedrock. Core correlation between XK08-A1 and XK08-A2 was carried out using surface scanning magnetic susceptibility in the laboratory. Subsequently, core XK08-A1 was split under subdued red light in the dark room and sectioned at 5–10 cm intervals for optically stimulated luminescence dating (OSL, Long et al., 2015). Core XK08-A2 was split into two halves. The core is mainly composed of fine-grained, grayish, minerogenic, organic-poor sediments, coarse sands appear at 251–255 cm deep (Sun et al., 2018). This study presents the geochemical results of Core XK08-A2, which was sectioned at 1 cm interval and the samples were stored at 4 °C in the repository prior to analysis. Radiocarbon dating using accelerator mass spectrometry may significantly underestimate the age of sediments for samples that were older than 30 cal kyr B.P., especially when sediments contain extremely

low organic matter, the chronology of Core XK08-A2 is mainly based on the correlation of the magnetic susceptibility with Core XK08-A1, where were dated using the OSL method (Sun et al., 2018).

3.2. Laboratory analyses

Every sample above 70 cm and 4-cm interval within others were selected for the geochemistry analysis, and five samples from the sandy ridges were also analyzed for comparison. All samples were freeze-dried, homogenized in an agate mortar, and then completely digested by HCl-HNO_3-HF-$HClO_4$ in Teflon beakers. The concentrations of major and minor elements (Al, K, Na, Mg, Ca, Fe, Ti, Mn and P) were determined using an inductively coupled plasma atomic emission spectrometer (ICP-AES) at the Analysis and Test center of Nanjing Institute of Geography and Limnology, Chinese Academy of Sciences. The data quality was guaranteed by using the analysis of reagent blanks, duplicate samples and standard reference materials (GBW07309) for each batch of samples. The standard deviations for determined values of the elements in standard reference materials were within ± 2% of the certified values.

3.3. Data processing

Chemical composition is compared with reference to the estimated element concentration in the upper continental crust (UCC) (Taylor and McLennan, 1995). To evaluate the element mobility, the elemental ratios (α values) for each element were calculated with reference to Al. This is because Al is considered to be stable during chemical weathering, diagenesis and not influenced by the biogeochemical processes (Garzanti et al., 2013; Singh et al., 2005). α value for any element *E* is defined as: $\alpha_{E} = (Al/E)_{sample}/(Al/E)_{UCC}$ (1). This ratio refers to the relative enrichment or depletion of the element, i.e. > 1 indicates depletion, < 1 indicates enrichment and =1 indicates no change in the relative abundance of element.

CIA (Nesbitt and Young, 1982) and weathering Index of Parker (WIP) (Parker, 1970) are the most widely used indices for silicate chemical weathering, and both defined as the molar proportions: $CIA = (Al_2O_3) / (Al_2O_3 + CaO^* + Na_2O + K_2O) \times 100$ (2); and $WIP = (CaO^*/0.7 + 2\ Na_2O/0.35 + 2\ K_2O/0.25 + MgO/0.9) \times 100$ (3). Where CaO^* represents the amount of CaO incorporated in the silicate minerals of samples, corrected following the method proposed by McLennan (1993). If the number of CaO moles after correcting for Ca in apatite is greater than that of Na_2O, we assume $CaO^* = Na_2O$, otherwise $CaO^* = CaO - 10/3\ P_2O_5$. CIA values are employed to quantitatively infer the degree of weathering and conversion of feldspars to secondary clay minerals in relative to fresh parent rocks (Nesbitt and Young, 1982). Although WIP value was suggested to be more applicable to weathering profiles on heterogeneous parent rocks or sediments, it was not applicable to highly weathered mantles (Parker, 1970; Price and Velbel, 2003).

4. Results

The basic statistics for major and minor elemental concentrations in the sediments of Lake Xingkai and surrounding sandy ridges are summarized in Table 1 and plotted in Fig. 2. Mean elemental concentrations follow the order Al > Fe > K > Na > Mg > Ca > Ti > Mn > P for lacustrine sediments, and Al > K > Na > Fe > Ca > Ti > P > Mn for the sandy ridges. Mn concentration exhibits the greatest change in both lacustrine sediments and sandy ridges, with the maximum coefficient of variation (CV) of 64% and 109%, respectively. Fe, Mg, Na and P concentrations also show significant fluctuations while Ca, K and Ti concentrations are relatively stable in the lacustrine sediments. However, Ca, Fe, Mg, P and Ti show significant variation in the sands from sandy ridges. Al-normalized ratios of K, Na and Ca all are related to the increase of coarse particles in the lacustrine sediments.

For the Al-normalized element ratios, Ca/Al, K/Al, Na/Al and Ti/Al ratios display similar fluctuations to grain-size variations, while Fe/Al and Mg/Al show negative correlations with the grain-size (Fig. 2). After normalized to the average chemical composition of the UCC, α values for Ca, Na, Mg, K and P of the bulk samples in the lacustrine sediments generally have values above 1 (with a mean of 3.53, 2.05, 1.59, 1.30 and 1.69, respectively, Fig. 3). The element ratios of Ti in all samples range from 0.39 to 0.62 with a mean of 0.54, and α values for Fe and Mn vary from 0.79 to 1.52 and from 0.16 to 1.71, respectively (Fig. 3). In contrast, α values for Ca, Na, Fe, Mg, P and Ti are > 1 in the sandy ridge sediments, while the element ratios of K range from 0.43 to 0.59 with a mean of 0.48 (Fig. 3).

The CIA values of the lacustrine sediments range from 55.5 to 70.3 with a mean of 65.3 (Fig. 2). On the basis of the correlated age with OSL dating, the sequence could be divided into three stages: the CIA values tend to be lower in the interglacial stages (MIS 5 and 1) than the last glaciation (MIS 4 to 2). During the last interglacial period, CIA values ranged from 59.1 to 69.4, with a mean of 65.1. During the last glaciation, they increased significantly during MIS 4 and early MIS 3, ranging from 64.8 to 70.3, with a mean of 68.3, while they ranged from 64.7 to 68.1 with a mean of 67.1 during MIS 2. During the Holocene, CIA values fluctuated frequently, ranging from 55.5 to 65.2, with a mean of 58.9. The WIP values, however, with an opposite trend, ranging from 42.4 to 50.8 with a mean of 45.5 (Fig. 2). CIA values of sandy ridged range from 51.8 to 54.7 with a mean of 52.6, which were significantly lower than that of the lacustrine sediments. While WIP values vary between 45.6 and 50.5 with a mean of 47.7, close to that of the lacustrine sediments.

5. Discussion

5.1. Chemical weathering history and origin of the offshore lacustrine sediments

Ca, and Na are generally easier to be depleted from the UCC, due to minerals enriched in Ca and Na (cacite, dolomite and plagioclase) are more fragile to chemical weathering. In contrast, K hosted in K-feldspars and mica, are more resistant to chemical weathering than plagioclase. Therefore, chemical weathering leads to the removal of Na and Ca during the early stage and K during intermediate stage (Nesbitt et al., 1980). In the sediments from Lake Xingkai, depletion of Ca and Na is evident, while K is less influenced comparing to UCC. The CIA values of the lacustrine samples are slightly higher than that of the UCC (47.9), fresh basalts (30–45), granites and granodiorites (45–55), and the surrounding sandy ridges (52.6), but lower than that of the terrestrial shale (70.4).This indicates that the sediment had undergone the primary stage of chemical weathering (Taylor and McLennan, 1995). Furthermore, the mean CIA value is close to the paleosol and higher than the loess in north China (Yang et al., 2006). On the A- CN- K diagram, terrestrial shale is the typical chemical weathering product of UCC, and the direction from UCC to terrestrial shale on the diagram represents the typical trend of continental chemical weathering, which is also parallel to the A- CN line (Nesbitt and Young, 1984). The data points of lacustrine sediments from Lake Xingkai were also parallel to the main trend of silicate weathering, and most of the investigated samples seem to be weathered from UCC, instead of directly from the rocks in the catchment (Fig. 4A).

The plot of Ti/Al vs. K/Al ratios has been proven very useful for tracing the province of sediments (Hao et al., 2010; Peng et al., 2016). Ti/Al ratio of sediment is initially determined by parent soil or rock type, because Ti content may be quite variable among different types of rocks even when Al content remains relative constant (Young and Nesbitt, 1998; Sheldon and Tabor, 2009; Hao et al., 2010). Moreover, Ti and Al are considered to be relatively immobile during chemical weathering and are inactive elements under early diagenesis. However,

Table 1
Chemical composition of lacustrine sediments in Lake Xingkai and surrounding sandy ridges compare with the UCC (Taylor and Mclennan, 1995).

		Al (mg/g)	Ca (mg/g)	Fe (mg/g)	K (mg/g)	Mg (mg/g)	Mn (mg/kg)	Na (mg/g)	P (mg/kg)	Ti (mg/g)
Lacustrine sediments	Max	87.2	9.6	50.8	22.2	11.0	3850.9	20.6	784.9	5.8
	Min	57.0	6.9	17.3	18.6	4.2	310.6	10.8	205.9	4.7
	Mean	77.9	8.3	34.3	20.8	8.4	653.4	14.2	411.8	5.4
	CV	0.10	0.04	0.21	0.04	0.21	0.64	0.17	0.21	0.03
Sandy ridges	Max	49.6	6.2	10.1	33.5	1.7	478.7	12.7	342.8	1.5
	Min	39.1	1.7	3.9	29.1	0.4	56.6	9.9	103.4	0.4
	Mean	43.7	3.6	5.9	31.7	0.7	165.1	11.1	165.7	0.8
	CV	0.10	0.47	0.41	0.05	0.74	1.09	0.10	0.60	0.62
UCC		80.4	30.0	35.0	28.0	13.3	600	28.9	700	3.0

some studies suggested that Ti/Al ratio could also be significantly influenced by the particle grain-size and dynamic of transportation due to two processes: the Ti-bearing minerals are more resistant to mechanical comminution, meanwhile, heavy minerals decline gradually as a result of gravity fractionation during transportation (Zabel et al., 1999; H. F. Chen et al., 2013; Peng et al., 2016). The ratio of K/Al could also be used to reflect the composition of the parent materials during the early stage of chemical weathering, due to that K is tightly bound in the clay particles and making it less mobile during chemical weathering of K-bearing silicate (Hao et al., 2010). The geochemical compositions demonstrated that the lacustrine sediments from Lake Xingkai can be clearly distinguished from sands from the sandy ridges nearby and clay fraction of loess from the Chinese Loess Plateau (Fig. 5). However, the lacustrine sediments from Lake Xingkai generally overlap with the range of values for the silt and sand fractions of loess from Chinese Loess Plateau, Harbin loess and the modern dust from northeast China (Fig. 5A, Yang et al., 2006; Xie and Chi, 2016; Xie et al., 2018). The similar ranges of Ti/Al and K/Al values for lacustrine sediments from Lake Xingkai and loess deposits in North China suggest that they come from broadly similar desert sources and atmospheric dust loading plays an important role in the lacustrine deposition.

In the Chinese Loess Plateau, Ti/Al ratios are similar across different grain-size fractions within the silt- and sand-sized particles, and only remarkably lower Ti/Al ratios occur in the clay fraction, resulting in rather uniform Ti/Al ratios for bulk samples from the Chinese Loess Plateau (Yang et al., 2006; Hao et al., 2010). In this study, however, higher Ti/Al ratios are related to increased coarse particles, and lower Ti/Al values are corresponding to increased fine particles (Fig. 6A). This difference may be attributed to different sorting mechanisms during wind transport and deposition processes of the aeolian sediment.

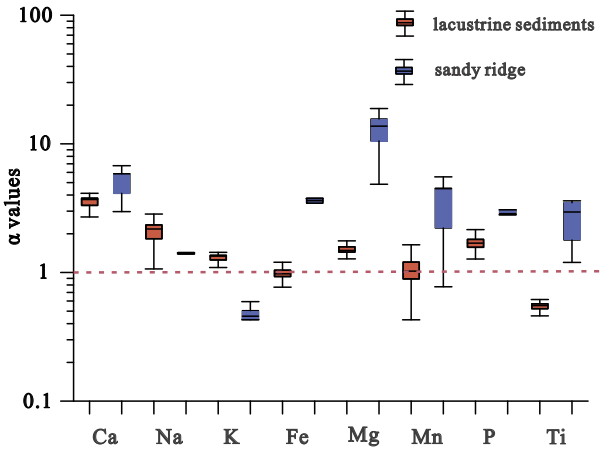

Fig. 3. Box-Whisker plots of the α values in sediments from Lake Xingkai and the surrounding sandy ridges.

Theoretically, the component of average grain-size < 10 μm is mainly transported by upper-level air flow in long-term suspension, while particles larger than 10 μm would be transported by surface winds to the distance about hundreds kilometers or rolled around in the source area (Tsoar and Pye, 1987; Sun et al., 2008). In addition, Lake Xingkai is blocked by Changbai Mountains and distant from the arid and semi-arid zones in north China and Mongolia Gobi in the west. The sand and coarse fractions mainly deposited in the west of Changbai Mountain while the catchment of Lake Xingkai is mainly influenced by fine dust, as indicated by the fact that the loess in northeast China is present to

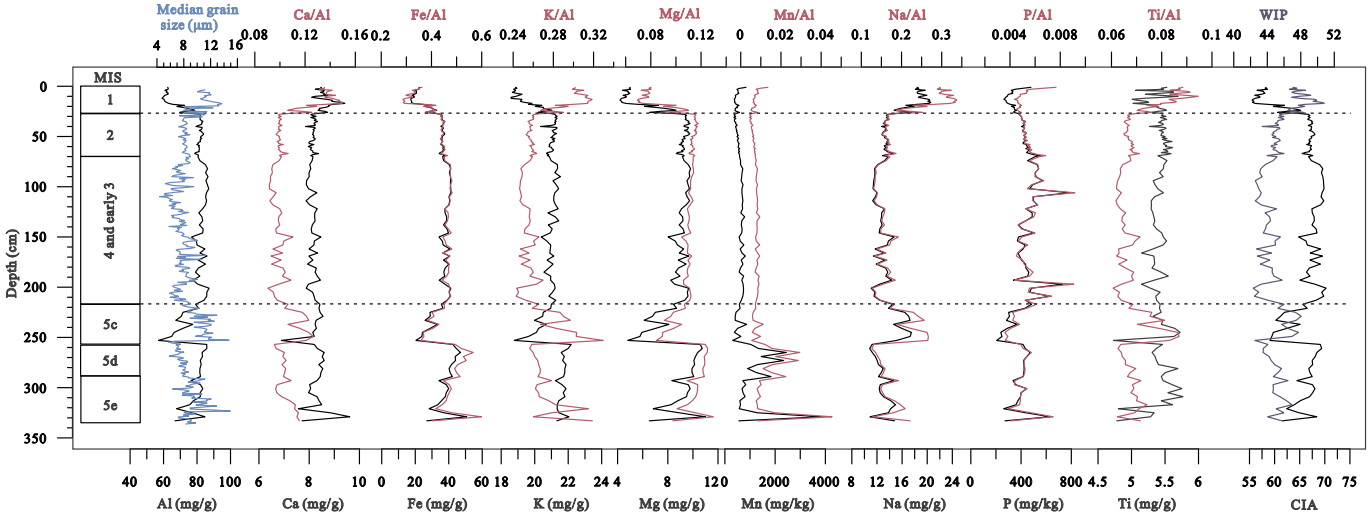

Fig. 2. Stratigraphy and variations in the median grain size (Sun et al., 2018, light blue curve), major element concentrations, Al-normalized ratios, CIA and WIP values of Core XK08-A2 sediments. (For interpretation of the references to colour in this figure legend, the reader is referred to the web version of this article.)

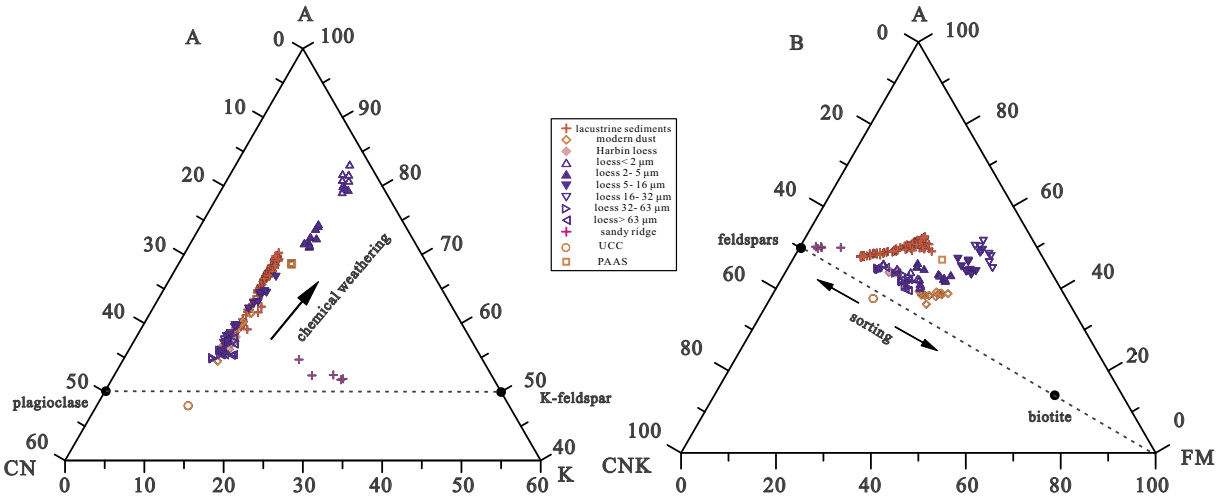

Fig. 4. A-CN-K (A) and A-CNK-FM (B) ternary diagrams characterizing weathering trend, sedimentary sorting and primitive minerals nature for the sediments from Lake Xingkai and the sandy ridges nearby. UCC and PASS (Taylor and McLennan, 1995) are also plotted, as well as multiple grain-size fractions of loess and paleosol deposits from the Chinese Loess Plateau (Yang et al., 2006), Harbin loess and modern dust samples from northeast China (Xie and Chi, 2016; Xie et al., 2018) for comparison. The arrow in (A) represents predicted weathering trend and in (B) represents the effect of grain-size sorting and sediments recycling.

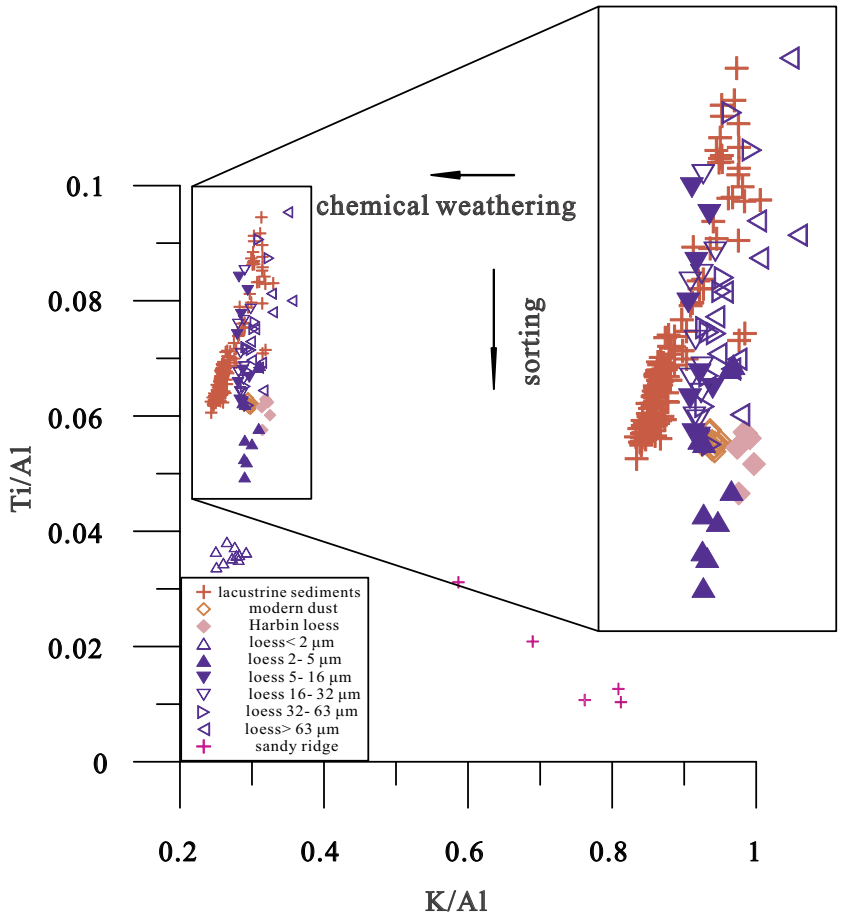

Fig. 5. Comparison of Ti/Al vs. K/Al ratios for the sediments from Lake Xingkai and the surrounding sandy ridges with multiple grain-size fractions of loess and paleosol deposits from the Chinese Loess Plateau (Yang et al., 2016), Harbin loess and modern dust samples from northeast China (Xie and Chi, 2016; Xie et al., 2018).

the west of the Great Xing'an Mountain and Changbai Mountain (Fig. 1A). Thus the provenance of the offshore lacustrine sediments was relatively stable and the Ti/Al ratiosare more sensitive to the grain-size distribution.

5.2. Effect of grain-size sorting and recycling on the chemical weathering indices

According to Eq. (2), CIA values primarily reflect the concentrations in mobile alkali and/or alkaline-earth metals relative to non-mobile aluminum in sediments, whereas WIP values reflect concentrations of Mg, Ca, Na, and K. In this study, Al-normalized ratios of K, Na and Ca

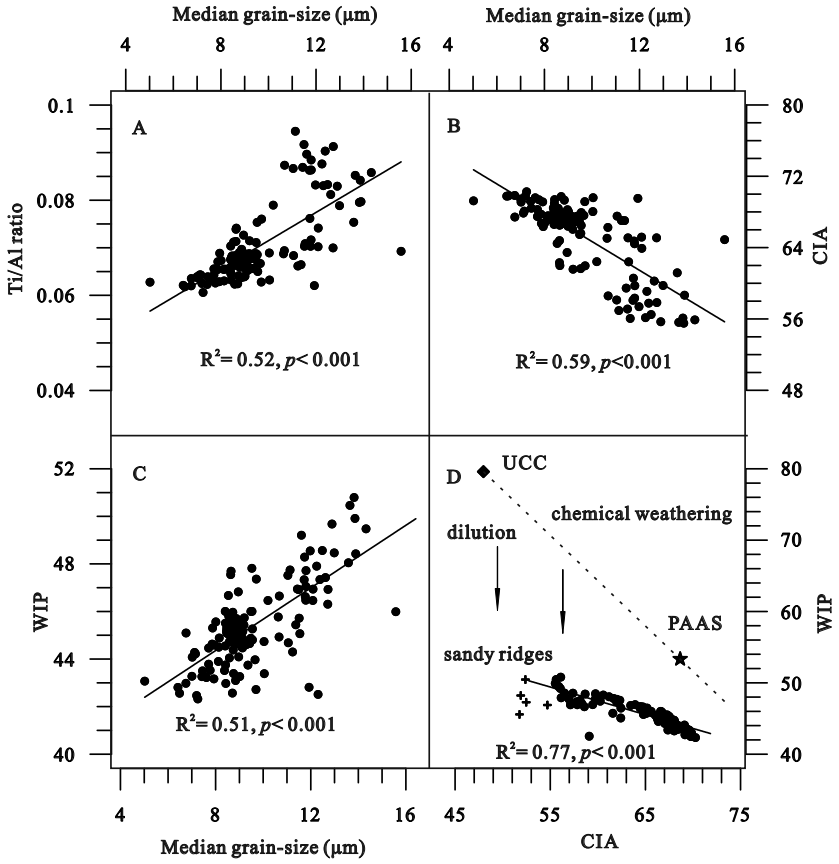

Fig. 6. Linear correlations between Ti/Al ratio (A), CIA (B), and WIP (C) values of the lacustrine sediments and corresponding grain-size (Sun et al., 2018), and discriminating polycyclic sediments with the chemical weathering indices, because quartz dilution affects strongly WIP but not CIA, the CIA/WIP plot readily reveals quartz enrichment in sediments (D, after Garzanti et al., 2013).

display similar fluctuations to Ti/Al variations, which are all related to the increase of coarse particles in the lacustrine sediments. In contrast, positive correlation is observed between median grain-size and concentration of Na, whereas negative correlations occur between median grain-size and concentration of Mg and K. Ca concentration shows no significant correlation with median grain-size. Therefore, the Lake Xingkai sediments show a good correlation between the median grain-size and the CIA values relative to the WIP values (Fig. 6B and C). Moreover, the CIA and WIP values in all samples correlate well, exhibiting greater CIA and smaller WIP values (Fig. 6D). These correlations suggest that these two weathering indices, despite their different methods to evaluate the weathering degree of the lacustrine sediments, can be significant influenced by sediment grain-size.

Significant impact of sediment grain-size on major element abundance and chemical weathering indices are also detected in some other studies. Nesbitt et al. (1996) found that the mud sediments have greater CIA values than the sands, primarily resulted from the intensive chemical weathering causing the destruction of the primary minerals and enrichment of secondary clay minerals in fine-grained sediments. Similarly, the CIA values of the finer suspended particulate matters from major rivers in China are overall greater than those in the corresponding floodplain sediments, and the values of clayey grain-size soils from east China are greater than those in the bulk samples (Shao et al., 2012; Qiu et al., 2014). Moreover, Yang et al. (2006) and Xiong et al. (2010) analyzed multiple grain-size fractions of loess and paleosol deposits from the Chinese Loess Plateau and showed that both the clayey fraction and fine-silt fractions had undergone greater chemical weathering intensity before deposition, indicating that the CIA values are strongly grain-size dependence. In comparison, the effect of grain-size on the WIP is ambiguous, for example, the WIP values display no significant correlation with the grain-size of suspended particulate matters and floodplain sediments from the Changjiang River Basin in China (Shao et al., 2012). The uncertainties maybe mainly due to that the WIP values are markedly affected by non-silicate minerals dilution, such as quartz, which is often more enriched in coarser particles (Fig. 6D).

To intuitively evaluate grain-size sorting and materials recycling on the geochemistry of the lacustrine sediments, the Al_2O_3- CaO^* + Na_2O $^+$ K_2O- Fe_2O_3 $^+$ MgO (A-CNK-FM) ternary diagram was proposed (Nesbitt et al., 1996). Overall, the distribution of the studied data is nearly parallel to the CNK-FM line, and obviously diverged from the typical trend of continental chemical weathering (Fig. 4B). The distribution pattern is consistent with multiple grain-size fractions of loess and paleosol deposits from the Chinese Loess Plateau, suggesting that the relative abundance of Ca, Na and K to Fe and Mg are also likely to be influenced by grain-size sorting associated with the sedimentary processes (Yang et al., 2006). Higher Ca/Al, K/Al and Na/Al ratios are related to coarse particles, and higher Fe/Al and Mg/Al values are corresponding to fine particles which maybe primary resulted from the comminution of mineral particles during transportation. Mica is comminuted to a greater extent than the feldspars due to that biotite is softer than the feldspars, although both have perfect cleavages (Nesbitt and Young, 1996). The recycling of aeolian sediments thus leads to further loss of mica and an increase in feldspars. In addition, Fe is redox-sensitive in aquatic environment, reducing conditions result in the release and recycling of Fe in the limnological ecosystem, which could lead to the different distribution of Lake Xingkai sediments from that of multiple grain-size fractions of loess and paleosol deposits from the Chinese Loess Plateau (Naeher et al., 2013).

5.3. Linkage between the Asian summer monsoon, physical erosion and chemical weathering indices

The record generally capture the variation of Asian summer monsoon on glacial- interglacial scale despite several sedimentary hiatuses, which occurred at 86.5 ± 11.2–65.5 ± 8.6, 53.3 ± 7.0–31.6 ± 4.1, 19 ± 2.5–8.2 ± 1.1 and 8.2 ± 1.1–0.4 ± 0.5 ka (Sun et al., 2018).

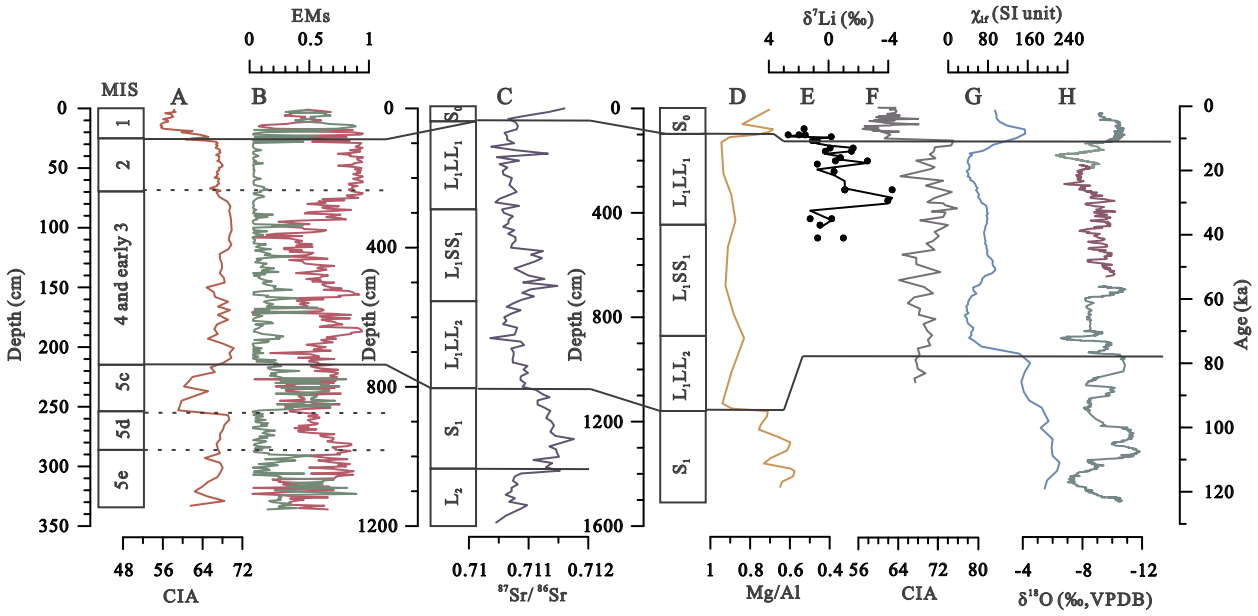

Fig. 7. Comparison of CIA record from Lake Xingkai (A) with other environments. (B) Fluvial transporting capacity derived from core XK08-A2 grain-size end members (green line represents the coarse particles transported by heavy runoff and pink line represents the fine particles transported by weakened runoff, Sun et al., 2018); (C) $^{87}Sr/^{86}Sr$ ratios of calcites in Luochuan loess-paleosol section (Yang et al., 2000); (D) Mg/Al ratios of the hydrochloric acid dissolvable fraction in Xifeng loess- paleosol section (Li et al., 2008); (E) Clay δ^7Li of terrace deposition in the Himalaya (Dosseto et al., 2015); (F) CIA values of the Zhuoshui River sediments in Taiwan (Zhao et al., 2017); (G) Magnetic susceptibility from Luochuan in Chinese Loess Plateau (An et al., 1991); (H) $\delta^{18}O$ records of stalagmite from Sanbao (light green) and Hulu (purple) Cave in east China (Wang et al., 2001; Wang et al., 2008). (For interpretation of the references to colour in this figure legend, the reader is referred to the web version of this article.)

These are in large part related to extreme droughts due to the weakened summer monsoon intensity, which triggered deflation and scouring of the lakebed. The dominant factors influence the chemical weathering indices of sediments including sediment sources, topographic settings, vegetation, and residence time of regolith within the basins, all are related to climate change (Yang et al., 2004; Yang et al., 2006; An et al., 2011).To illustrate the environmental implication of geochemical compositions of the Lake Xingkai sediments since the last interglacial period, we compare the CIA values of Core XK08-A2 with other chemical weathering indices and the widely-used paleomonsoon indicators in the Asian summer monsoon region (Fig. 7), including stalagmite oxygen isotope ($\delta^{18}O$) (Wang et al., 2001; Wang et al., 2008), magnetic susceptibility from the Chinese Loess Plateau (An et al., 1991).

A close link between glacial-interglacial Asian summer monsoon intensity and Lake Xingkai sediment geochemistry can be observed by comparing the CIA values with the stalagmite $\delta^{18}O$ records and magnetic susceptibility from the Chinese Loess Plateau (Fig. 7). Higher CIA values are related to weaker Asian summer monsoon and reduced precipitation during the glacial periods, while the lower CIA values are corresponding to strengthened Asian summer monsoon and increased precipitation during the interglacial periods. The results of this study are consistent with recent studies from the Himalayan range and Taiwan Strait, which suggested that silicate chemical weathering in mountainous areas was significantly inhibited by strengthened Asian summer monsoon (Dosseto et al., 2015; Zhao et al., 2017). The observations on the degree of sedimentary silicate weathering and Asian summer monsoon, however, are different to the records from the Chinese Loess Plateau, as the latter supports that chemical weathering and soil pedogenisis were enhanced by warmer and wetter climate conditions (Chen et al., 1999; Yang et al., 2000; Li et al., 2008).

Previous studies have suggested that monsoon intensification may result in increase of physical erosion rates via increased runoff and fluvial incision in high mountainous areas (Clift, 2006; Clift et al., 2014; Dosseto et al., 2015; Zhao et al., 2017). The average sedimentation rate was higher during the last glacial period than the interglacial periods, however, the pattern was disturbed by deflation and scouring of the lakebed which might not reflect soil erosion in the catchment (Long et al., 2015). The hydraulic dynamics of Lake Xingkai was strengthened during the last interglacial period and Holocene (Sun et al., 2018). Increased physical erosion might lead to reduced sediment residence time in the catchment, which in turn would have limited chemical weathering. In contrary, weakened Asian summer monsoon during the late glacial period would cause weakened runoff transporting capacity and a longer residence time of detritus in the mountainous basins. Consequently relatively slow sediment transfer rate and higher silicate weathering intensity was resulted.

It seems that lengthened residence time and strengthened silicate chemical weathering could explain the high CIA values during the last glacial period. However, considering the small amplitudes of special grain-size fraction CIA values between loess and paleosol horizons in the Chinese Loess Plateau, it is estimated that the pedogenic alteration are less significant than sediment sorting (Yang et al., 2006; Xiong et al., 2010). Our data show that the silicate weathering values are also significantly grain-size dependent, whereas changes in the CIA values of the core sediments are more likely to representing the sorting and recycling of the detritus in the Lake Xingkai catchment. Uranium isotope disequilibria was analyzed in the river sediments from Asia, the transport time of sediments from source to sink might vary from 20 kyr in the Ganges River and its main tributaries in south Asia to about 600 kyr in the Yangtze River in China (Granet et al., 2007; Granet et al., 2010; Li et al., 2016). Similarly, the transport time of the aeolian deposits from the arid inland basins to the Chinese Loess Plateau was about 240 kyr estimated by Uranium isotope disequilibria method (Li et al., 2017). In addition, Beaulieu et al. (2012) have shown that the chemical weathering is dominated by carbonate weathering on the decadal to centennial scale. Therefore, the silicate weathering degrees of Lake Xingkai sediments might have reflected the effects of integrated weathering and diagenetic histories, instead of directly or instantaneously responded to the catchment chemical weathering on the glacial-interglacial timescale. During the last glacial period, the dominant modal size of

recycled aeolian sediments transported by rivers was about 10 μm, in addition, abundant fine silt dust was transported into the lake by the westerlies during MIS 4 and the early MIS 3 (Sun et al., 2018). The higher atmospheric dust loading and weakened runoff consequently resulted in higher weathering degree sediments in the lake basin. In contrary, enhanced East Asian summer monsoon during the last interglacial period and Holocene limited the dust emission in the arid inland, and the heavy runoff transported the coarser and less-weathered detritus into the lake (Fig. 7).

6. Conclusions

In this study, we performed major element analyses on 136 lacustrine samples and five sand samples from Lake Xingkai and the surrounding sandy ridges in northeast China. The results indicate that their abundance in the lacustrine sediments varied in relatively narrow ranges. UCC-normalized element abundance show evident depletions of Ca and Na, while Ti is enriched. The lower CIA values of the lacustrine samples indicate that the sediments had only undergone the primary stage of chemical weathering. On the A-CN-K diagram and Ti/Al vs K/Al plot, similar patterns between the lacustrine samples from Lake Xingkai and the loess-paleosol samples in north China suggest that the lacustrine samples from Lake Xingkai are likely lacustro-aeolian deposits (reworked or mixed, loess derived sediment), rather than directly derived from the bedrock detritus in the catchment. Correlation analyses of grain-size and chemical weathering indices indicate that CIA and WIP values are strongly related to grain-size of particles and sediments recycling. Finally, the chemical weathering indices of the lacustrine sediments reflected the effects of integrated weathering and diagenetic histories in the mid-latitudes of Northern Hemisphere. CIA values of the lacustrine sediments might be linked to climate change through the development of runoff and physical erosion in the catchment and the dust emission in the arid inland basins in north China. Higher CIA values are corresponding to weakened Asian summer monsoon whereas lower CIA values are related to strengthened Asian summer monsoon. This study provides an insight into sedimentary response to Asian summer monsoon changes in Lake Xingkai during the late Quaternary, helping us to better understand the earth surface processes in the mid-latitudes of Northern Hemisphere.

Acknowledgments

We want to thank the editor and two anonymous reviewers for helpful comments that improved the quality of this manuscript. We also would like to express our gratitude to Dr. Y. Wang for field assistance. This research was supported by the National Natural Science Foundation of China (Grant Nos. 41430530, 41621002 and 41702183) and the National Key R&D Program of China (Grant 2017YFA0605203).

References

An, Z., Kukla, G.J., Porter, S.C., Xiao, J., 1991. Magnetic susceptibility evidence of monsoon variation on the Loess Plateau of central China during the last 130,000 years. Quat. Res. 36, 29–36.
An, Z., Clemens, S.C., Shen, J., Qiang, X., Jin, Z., Sun, Y., Prell, W.L., Luo, J., Wang, S., Xu, H., Cai, Y., Zhou, W., Liu, X., Liu, W., Shi, Z., Yan, L., Xiao, X., Chang, H., Wu, F., Ai, L., Lu, F., 2011. Glacial-interglacial Indian summer monsoon dynamics. Science 333, 719–723.
Ao, H., Deng, C., Dekkers, M.J., Sun, Y., Liu, Q., Zhu, R., 2010. Pleistocene environmental evolution in the Nihewan Basin and implication for early human colonization of North China. Quat. Int. 223-224, 472–478.
Beaulieu, E., Goddéris, Y., Donnadieu, Y., Labat, D., Roelandt, C., 2012. High sensitivity of the continental-weathering carbon dioxide sink to future climate change. Nat. Clim. Chang. 2, 346–349.
Cai, M., Wei, M., Yang, Y., Wang, J., Xu, D., 2014. Long-term cooling/drying record of North China since the middle Pleistocene from geochemical evidence of a 150 m deep drill core, Beijing plain, China. Quat. Int. 349, 419–427.
Chen, J., An, Z., Head, J., 1999. Variation of Rb/Sr ratios in the Loess-Paleosol sequences of Central China during the last 130,000 years and their implications for monsoon paleoclimatology. Quat. Res. 51, 215–219.
Chen, F., Qiang, M., Zhou, A., Xiao, S., Chen, J., Sun, D., 2013. A 2000-year dust storm record from Lake Sugan in the dust source area of arid China. J. Geophys. Res. Atmos. 118, 2149–2160.
Chen, H.-F., Yeh, P.-Y., Song, S.-R., Hsu, S.-C., Yang, T.-N., Wang, Y., Chi, Z., Lee, T.-Q., Chen, M.-T., Cheng, C.-L., Zou, J., Chang, Y.-P., 2013. The Ti/Al molar ratio as a new proxy for tracing sediment transportation processes and its application in aeolian events and sea level change in East Asia. J. Asian Earth Sci. 73, 31–38.
Clift, P.D., 2006. Controls on the erosion of Cenozoic Asia and the flux of clastic sediment to the ocean. Earth Planet. Sci. Lett. 241, 571–580.
Clift, P.D., Wan, S., Blusztajn, J., 2014. Reconstructing chemical weathering, physical erosion and monsoon intensity since 25 Ma in the northern South China Sea: a review of competing proxies. Earth Sci. Rev. 130, 86–102.
Dosseto, A., Vigier, N., Joannes-Boyau, R., Moffat, I., Singh, T., Srivastava, P., 2015. Rapid response of silicate weathering rates to climate change in the Himalaya. Geochem. Perspect. Lett. 1, 10–19.
Garzanti, E., Padoan, M., Setti, M., Najman, Y., Peruta, L., Villa, I.M., 2013. Weathering geochemistry and Sr-Nd fingerprints of equatorial upper Nile and Congo muds. Geochem. Geophys. Geosyst. 14, 292–316.
Granet, M., Chabaux, F., Stille, P., France-Lanord, C., Pelt, E., 2007. Time-scales of sedimentary transfer and weathering processes from U-series nuclides: clues from the Himalayan rivers. Earth Planet. Sci. Lett. 261, 389–406.
Granet, M., Chabaux, F., Stille, P., Dosseto, A., France-Lanord, C., Blaes, E., 2010. U-series disequilibria in suspended river sediments and implication for sediment transfer time in alluvial plains: the case of the Himalayan rivers. Geochim. Cosmochim. Acta 74, 2851–2865.
Hao, Q., Guo, Z., Qiao, Y., Xu, B., Oldfield, F., 2010. Geochemical evidence for the provenance of middle Pleistocene loess deposits in southern China. Quat. Sci. Rev. 29, 3317–3326.
Hu, D., Böning, P., Köhler, C.M., Hillier, S., Pressling, N., Wan, S., Brumsack, H.J., Clift, P.D., 2012. Deep sea records of the continental weathering and erosion response to East Asian monsoon intensification since 14 ka in the South China Sea. Chem. Geol. 326–327, 1–18.
Jiang, H., Guo, G., Cai, X., Thompson, J.A., Xu, H., Zhong, N., 2016. Geochemical evidence of windblown origin of the late Cenozoic lacustrine sediments in Beijing and implications for weathering and climate change. Palaeogeogr. Palaeoclimatol. Palaeoecol. 446, 32–43.
Jin, Z.D., Wang, S.M., Shen, J., Zhang, E.L., Li, F.C., Ji, J.F., Lu, X.W., 2001. Chemical weathering since the little ice age recorded in lake sediments: a high-resolution proxy of past climate. Earth Surf. Process. Landf. 26, 775–782.
Jin, Z., An, Z., Yu, J., Li, F., Zhang, F., 2015. Lake Qinghai sediment geochemistry linked to hydroclimate variability since the last glacial. Quat. Sci. Rev. 122, 63–73.
Kump, L.R., Brantley, S.L., Arthur, M.A., 2000. Chemical weathering, atmospheric CO_2, and climate. Annu. Rev. Earth Planet. Sci. 28, 611–667.
Li, G., Ji, J., Zhao, L., Mao, C., Chen, J., 2008. Response of silicate weathering to monsoon changes on the Chinese loess plateau. Catena 72, 405–412.
Li, C., Yang, S., Zhao, J.-x., Dosseto, A., Bi, L., Clark, T.R., 2016. The time scale of river sediment source-to-sink processes in East Asia. Chem. Geol. 446, 138–146.
Li, L., Liu, X., Li, T., Li, L., Zhao, L., Ji, J., Chen, J., Li, G., 2017. Uranium comminution age tested by the eolian deposits on the Chinese Loess Plateau. Earth Planet. Sci. Lett. 467, 64–71.
Liu, X., Dong, H., Yang, X., Herzschuh, U., Zhang, E., Stuut, J.-B.W., Wang, Y., 2009. Late Holocene forcing of the Asian winter and summer monsoon as evidenced by proxy records from the northern Qinghai–Tibetan Plateau. Earth Planet. Sci. Lett. 280, 276–284.
Liu, J., Chen, J., Selvaraj, K., Xu, Q., Wang, Z., Chen, F., 2014. Chemical weathering over the last 1200 years recorded in the sediments of Gonghai Lake, Lvliang Mountains, North China: a high-resolution proxy of past climate. Boreas 43, 914–923.
Long, H., Shen, J., 2017. Sandy beach ridges from Xingkai Lake (NE Asia): timing and response to palaeoclimate. Quat. Int. 430, 21–31.
Long, H., Shen, J., Wang, Y., Gao, L., Frechen, M., 2015. High-resolution OSL dating of a late quaternary sequence from Xingkai Lake (NE Asia): chronological challenge of the "MIS 3a mega-paleolake" hypothesis in China. Earth Planet. Sci. Lett. 428, 281–292.
Mclennan, S.M., 1993. Weathering and global denudation. J. Geol. 101 (2), 295–303.
Naeher, S., Gilli, A., North, R.P., Hamann, Y., Schubert, C.J., 2013. Tracing bottom water oxygenation with sedimentary Mn/Fe ratios in Lake Zurich, Switzerland. Chem. Geol. 352, 125–133.
Nesbitt, H.W., Young, G.M., 1982. Early Proterozoic climate and plate motions inferred from major element chemistry of lutites. Nature 299, 715–717.
Nesbitt, H.W., Young, G.M., 1984. Prediction of some weathering trends of plutonic and volcanic rocks based on thermodynamic and kinetic considerations. Geochim. Cosmochim. Acta 48, 1523–1534.
Nesbitt, H.W., Young, G.M., 1996. Petrogenesis of sediments in the absence of chemical weathering: effects of abrasion and sorting on bulk composition and mineralogy. Sedimentology 43, 341–358.
Nesbitt, H.W., Markovics, G., Price, R.C., 1980. Chemical processes affecting alkalis and alkaline earths during continental weathering. Geochim. Cosmochim. Acta 44, 1659–1666.
Nesbitt, H.W., Young, G.M., Mclennan, S.M., Keays, R.R., 1996. Effects of chemical weathering and sorting on the petrogenesis of siliciclastic sediments, with implications for provenance studies. J. Geol. 104, 525–542.
Parker, A., 1970. An index of weathering for silicate rocks. Geol. Mag. 107, 501–504.
Peng, S., Hao, Q., Wang, L., Ding, M., Zhang, W., Wang, Y., Guo, Z., 2016. Geochemical and grain-size evidence for the provenance of loess deposits in the Central Shandong Mountains region, northern China. Quat. Res. 85, 290–298.
Price, J.R., Velbel, M.A., 2003. Chemical weathering indices applied to weathering profiles developed on heterogeneous felsic metamorphic parent rocks. Chem. Geol. 202,

397–416.
Qiu, S., Zhu, Z., Yang, T., Wu, Y., Bai, Y., Ouyang, T., 2014. Chemical weathering of monsoonal eastern China: implications from major elements of topsoil. J. Asian Earth Sci. 81, 77–90.
Rogers, J.R., Bennett, P.C., Choi, W.J., 1998. Feldspars as a source of nutrients for microorganisms. Am. Mineral. 83, 1532–1540.
Selvaraj, K., Chen, C.T.A., Lou, J.-Y., 2007. Holocene East Asian monsoon variability: Links to solar and tropical Pacific forcing. Geophys. Res. Lett. 34.
Shao, J., Yang, S., Li, C., 2012. Chemical indices (CIA and WIP) as proxies for integrated chemical weathering in China: inferences from analysis of fluvial sediments. Sediment. Geol. 265–266, 110–120.
Sheldon, N.D., Tabor, N.J., 2009. Quantitative paleoenvironmental and paleoclimatic reconstruction using paleosols. Earth Sci. Rev. 95, 1–52.
Shen, J., 2013. Spatiotemporal variations of Chinese lakes and their driving mechanisms since the Last Glacial Maximum: a review and synthesis of lacustrine sediment archives. Chin. Sci. Bull. 58, 17–31.
Singh, M., Sharma, M., Tobschall, H.J., 2005. Weathering of the Ganga alluvial plain, northern India: implications from fluvial geochemistry of the Gomati River. Appl. Geochem. 20, 1–21.
Sun, D., Su, R., Bloemendal, J., Lu, H., 2008. Grain-size and accumulation rate records from Late Cenozoic aeolian sequences in northern China: implications for variations in the East Asian winter monsoon and westerly atmospheric circulation. Palaeogeogr. Palaeoclimatol. Palaeoecol. 264, 39–53.
Sun, W., Shen, J., Yu, S., Long, H., Zhang, E., Liu, E., Chen, R., 2018. A lacustrine record of East Asian summer monsoon and atmospheric dust loading since the last interglaciation from Lake Xingkai, NE China. Quat. Res. 89, 270–280.
Taylor, S.R., McLennan, S.M., 1995. The geochemical evolution of the continental crust. Rev. Geophys. 33, 241–265.
Tsoar, H., Pye, K., 1987. Dust transport and the question of desert loess formation. Sedimentology 34, 139–153.
Uno, I., Eguchi, K., Yumimoto, K., Takemura, T., Shimizu, A., Uematsu, M., Liu, Z., Wang, Z., Hara, Y., Sugimoto, N., 2009. Asian dust transported one full circuit around the globe. Nat. Geosci. 2, 557–560.
Wan, B., Zhong, Y., 1997. Features analysis and divisions of new tectonic movement in Northeast China. Seismol. Res. Northeast China 13 (4), 64–75 (in Chinese).
Wang, Y.J., Cheng, H., Edwards, R.L., An, Z.S., Wu, J.Y., Shen, C.-C., Dorale, J.A., 2001. A high-resolution absolute-dated late Pleistocene monsoon record from Hulu Cave, China. Science 294, 2345–2348.
Wang, Y., Cheng, H., Edwards, R.L., Kong, X., Shao, X., Chen, S., Wu, J., Jiang, X., Wang, X., An, Z., 2008. Millennial- and orbital-scale changes in the East Asian monsoon over the past 224,000 years. Nature 451, 1090–1093.
Williams, D.F., Kuzmin, M.I., Prokopenko, A.A., et al., 2001. The Lake Baikal drilling project in the context of a global lake drilling initiative. Quat. Int. 80–81, 3–18.
Xiao, J.L., An, Z.S., Liu, T.S., Inouchi, Y., Kumai, H., Yoshikawa, S., Kondo, Y., 1999. East Asian monsoon variation during the last 130,000 years: evidence from the Loess Plateau of central China and Lake Biwa of Japan. Quat. Sci. Rev. 18, 147–157.
Xie, Y., Chi, Y., 2016. Geochemical investigation of dry- and wet-deposited dust during the same dust-storm event in Harbin, China: constraint on provenance and implications for formation of aeolian loess. J. Asian Earth Sci. 120, 43–61.
Xie, Y., Yuan, F., Zhan, T., Kang, C., Chi, Y., 2018. Geochemical and isotopic characteristics of sediments for the Hulun Buir Sandy Land, northeast China: implication for weathering, recycling and dust provenance. Catena 160, 170–184.
Xiong, S., Ding, Z., Zhu, Y., Zhou, R., Lu, H., 2010. A ~6Ma chemical weathering history, the grain size dependence of chemical weathering intensity, and its implications for provenance change of the Chinese loess–red clay deposit. Quat. Sci. Rev. 29, 1911–1922.
Yang, J., Chen, J., An, Z., Shields, G., Tao, X., Zhu, H., Ji, J., Chen, Y., 2000. Variations in $^{87}Sr/^{86}Sr$ ratios of calcites in Chinese loess: a proxy for chemical weathering associated with the East Asian summer monsoon. Palaeogeogr. Palaeoclimatol. Palaeoecol. 157, 151–159.
Yang, S., Jung, H.-S., Li, C., 2004. Two unique weathering regimes in the Changjiang and Huanghe drainage basins: geochemical evidence from river sediments. Sediment. Geol. 164, 19–34.
Yang, S., Ding, F., Ding, Z., 2006. Pleistocene chemical weathering history of Asian arid and semi-arid regions recorded in loess deposits of China and Tajikistan. Geochim. Cosmochim. Acta 70, 1695–1709.
Yang, H., Ge, W., Zhao, G., Yu, J., Zhang, Y., 2015. Early Permian–Late Triassic granitic magmatism in the Jiamusi–Khanka Massif, eastern segment of the Central Asian Orogenic Belt and its implications. Gondwana Res. 27, 1509–1533.
Young, G.M., Nesbitt, H.W., 1998. Processes controlling the distribution of Ti and Al in weathering profiles, siliciclastic sediments and sedimentary rocks. J. Sediment. Res. 68, 448.
Zabel, M., Bickert, T., Dittert, L., Haese, R.R., 1999. Significance of the sedimentary Al/Ti ratio as an indicator for variations in the circulation patterns of the equatorial North Atlantic. Paleoceanography 14, 789–799.
Zhao, L., Ji, J., Chen, J., Liu, L., Chen, Y., Balsam, W., 2005. Variations of illite/chlorite ratio in Chinese loess sections during the last glacial and interglacial cycle: Implications for monsoon reconstruction. Geophys. Res. Lett. 32.
Zhao, Y., Yang, S., Liu, J.T., Fan, D., Yang, R.J., Bi, L., Chang, Y.-p., 2017. Reconstruction of silicate weathering intensity and paleoenvironmental change during the late Quaternary in the Zhuoshui River catchment in Taiwan. Quat. Int. 452, 43–53.
Zhu, Y., Shen, J., Lei, G., Wang, Y., 2011. Environmental evolution of Xingkai (Khanka) Lake since 200 ka by OSL dating of sand hills. Chin. Sci. Bull. 56, 2604–2612.